International Journal of Cast Metals Research

ISSN: 1364-0461 (Print) 1743-1336 (Online) Journal homepage: http://www.tandfonline.com/loi/ycmr20

Effect of pressure on solidification of metallic materials

J J Sobczak, L Drenchev & R Asthana

To cite this article: J J Sobczak, L Drenchev & R Asthana (2012) Effect of pressure on solidification of metallic materials, International Journal of Cast Metals Research, 25:1, 1-14, DOI: 10.1179/1743133611Y.0000000016

To link to this article: http://dx.doi.org/10.1179/1743133611Y.0000000016

REVIEW

Effect of pressure on solidification of metallic materials

J. J. Sobczak[1], L. Drenchev[2] and R. Asthana*[3]

The effect of pressure on solidification structure formation in metal castings has been reviewed and explicitly expressed by thermodynamic relationships. In particular, pressure effects on phase diagrams, nucleation and growth, interfacial energy and diffusion coefficient are considered and analysed. Well known formulae and some new explicit relations are presented and discussed. Practical manifestations of the effect of pressure in casting structure formation are discussed.

Keywords: Solidification, Pressure, Thermodynamics, Free energy, Microstructure, Nucleation, Diffusion, Metal casting, Review

List of symbols

a, b	constants, Pa^{-1}
A	coefficient, J Pa^{-1}
B	constant, m^2 s^{-1}
c_p, c_{p1}, c_{p2}	specific heat capacity, J kg^{-1} K^{-1}
C	concentration, %
C_{eq}, $C_{eq,0}$	equilibrium concentrations, %
C_P	heat capacity of system, J K^{-1}
D	diffusion coefficient, m^2 s^{-1}
D_0	diffusion coefficient at pressure P_0, m^2 s^{-1}
g_1, g_2	molar Gibbs free energy, J mol^{-1}
G	Gibbs free energy, J
h	Planck's constant, $6{\cdot}626176 \times 10^{-34}$ J s
k_b	Boltzmann's constant, $1{\cdot}380662 \times 10^{-23}$ J K^{-1}
k_T	isothermal compressibility, Pa^{-1}
$l_{1\rightarrow2}$	molar latent heat, J mol^{-1}
L	latent heat of fusion, J m^{-3}
N	nucleation rate, s^{-1} m^{-3}
N_S	number of nucleation sites in unit volume, m^{-3}
P, P_0	pressures, Pa
r^*	critical radius for nucleation, m
s_1, s_2	molar entropy, J mol^{-1} K^{-1}
S	entropy, J K^{-1}
S_f	shape factor
S_m	molar entropy, J mol^{-1} K^{-1}
T	temperature, K
T_{eq}, $T_{eq,0}$	equilibrium temperatures for phase transformation, K
T_{eut}	eutectic temperature, K
T_m, T_0	melting temperatures, K
v, v_1, v_2	molar volumes, m^3 mol^{-1}
V	volume, m^{-3}
V_m	molar volume, m^3 mol^{-1}
V_m^0	molar volume at given pressure P_0, m^3 mol^{-1}
α, β, γ	different phases in a substance
ΔG_m	activation energy for migration of atoms, J mol^{-1}
ΔP	pressure increment, Pa
Δs	increment of molar entropy, J mol^{-1} K^{-1}
ΔT	melt undercooling $T_m - T$, K
Δv	increment of molar volume, m^3 mol^{-1}
ΔV_m	change in molar volume, m^3 mol^{-1}
ε	temperature increment, K
μ	chemical potential, J mol^{-1}
μ_0	chemical potential at given pressure P_0, J mol^{-1}
σ, $\sigma_{\alpha\beta}$	surface tension for α/β interfaces, J m^{-2}
χ, χ_1, χ_2	coefficients of thermal expansion, $(1/V)(\partial V/\partial T)_P$, K^{-1}

Introduction

Modern interest in the effect of pressure on the structure and properties of matter can be traced to the seminal work of Nobel Laureate physicist P. W. Bridgman.[1] Bridgman developed techniques to achieve high pressures ($\sim$10 GPa) and investigated pressure effects on thermal and electrical conductivities, melting, reaction kinetics, viscosity, compressibility, tensile strength and a variety of other properties and phenomena. Bridgman's work demonstrated the importance of pressure for studying continuous and discontinuous changes in the structure and properties of matter. His scientific results and engineering solutions have found a very large number of practical applications.

One of the most intriguing predictions concerning the effect of pressure was J. D. Bernal's suggestion that all matter should ultimately become metallic at sufficiently high pressure as the forced overlap of electron orbits will induce electron delocalisation.[2] More than 30 years after Bernal's prediction of 1928, high pressure transformation from insulator to metal was achieved in iodine, silicon, germanium and other elements.[3,4] Subsequently, metallisation was realised in other elements, including gases such as xenon and oxygen,[5] as well as in numerous molecular, ionic and covalent compounds.[4] In 1996,

[1]Foundry Research Institute, 73 Zakopianska street, 30–418 Krakow, Poland
[2]Institute of Metal Science, 67 Shipchenski Prohod street, 1574 Sofia, Bulgaria
[3]Department of Engineering and Technology, University of Wisconsin-Stout, 326 Fryklund Hall, Menomonie, WI 54751, USA

*Corresponding author, email AsthanaR@uwstout.edu

Received 4 January 2011; accepted 20 June 2011
DOI 10.1179/1743133611Y.0000000016

metallic hydrogen was obtained above 3700°C under a pressure of 140 GPa.[6]

Nature offers remarkable diversity and a range of pressure across length scales. On the earth's surface, the atmospheric pressure is ~0·1 MPa; in the earth's core, pressures are on the order of $\sim 3{\cdot}5 \times 10^2$ GPa; in the core of the sun, pressures are $\sim 2{\cdot}1 \times 10^7$ GPa; in white dwarfs, the pressure is 10^9–10^{12} GPa; and in pulsars, the pressure is on the order of 10^{20} GPa. In technical equipment, a limiting pressure of ~15 GPa can be achieved. The maximum static pressure realised in scientific experiments is near 3×10^2 GPa, and the dynamic pressure obtained by explosion reaches values of up to 30×10^2 GPa. Pressures higher than the atmospheric, which are used in engineering practice, can be divided conditionally into elevated pressures (up to 0·1 GPa) and high pressures (above this value).

In a statistical–mechanical sense, pressure reflects the impulse transferred upon collisions between gas molecules and is proportional to particle concentration (in contrast, temperature is proportional to the average kinetic energy). Pressure changes either force the atoms closer together in a small volume or give them more space to reside. Thus, pressure is a versatile variable to synthesise new structures and to investigate the nature of chemical bond and atomic interactions.

High pressures offer new pathways for phase transformation (e.g. solidification) and permit stable or metastable equilibrium states to be achieved. The classic example of this is the couple graphite and diamond at room temperature and atmospheric pressure. Graphite and diamond represent two states, one stable and the other metastable (in time, all diamonds will transform into graphite).

In casting technology, application of pressure allows effective melt transfer as well as modulation of the solidification process to generate new structures and materials. There are two ways that pressure affects casting solidification and structure formation: mechanical effects related to the physical phenomena at macrolevel (elastic and/or plastic deformation, intensification of heat exchange between casting and mould, variation of cooling rate, control of mould filling, etc.) and thermodynamic and transport phenomena at microlevel (changes in phase diagrams, physical properties, Gibbs free energy, chemical potentials, specific heat, surface tension, diffusion coefficients, etc). The physical phenomena at both macro- and microscales alter some basic thermodynamic and kinetic parameters of systems and, thus, influence phase transformations in the system. The main parameters in pressure application are magnitude of pressure, manner of its application to solidifying melt, durability of pressure influence and physical status of melt before application of the pressure.

Pressures in excess of the atmospheric can be applied to solidifying melts using either gas or specific mechanical systems (e.g. piston or plunger mechanisms). Conventional autoclaves or their variants are usually used for solidification under elevated gas pressure. Units with one or more plungers are designed for direct application of pressure on solidifying melt. Pressure can be applied during melt preparation (melting and alloying), melt transfer (mould filling), at the commencement of casting solidification, just before the end of solidification, or after solidification of entire casting but before its complete cooling (i.e. when casting temperature is less than but close to solidus temperature). On the other hand, melt can be overheated or cooled below the liquidus to form semisolid slurry before pressurisation.

Conventional casting technologies that make use of pressure are often based on purely empirical knowledge rather than sound design criteria that originate in an understanding of the physical changes caused by pressure. Understanding the entire complex of physical phenomena that accompany solidification under high pressure is facilitated by their thermodynamic and kinetic descriptions. This paper has the dual but complementary objectives of examining the effect of pressure on thermodynamic and kinetic factors important in solidification and practical manifestations of such effects in casting structure formation. Formulae from classical thermodynamics for pressure effects on equilibrium diagrams, phase nucleation, interfacial free energy, chemical potential and entropy are presented and discussed. Some new explicit relationships are also presented, and their implication to solidification under pressure is discussed.

Thermodynamics

The variation in Gibbs free energy when both temperature and pressure change for a system of fixed mass and composition can be expressed by the relation

$$\mathrm{d}G = -S\mathrm{d}T + V\mathrm{d}P \tag{1}$$

At constant temperature, $\mathrm{d}T=0$, and equation (1) transforms to

$$\left(\frac{\partial G}{\partial P}\right)_{\mathrm{T}} = V \tag{2}$$

i.e. at constant temperature, the free energy of a phase increases with the increase in pressure at a rate V. The equation leads to the fact that an increase in pressure could promote the formation of new phase with a smaller molar volume. More detailed reviews of the free energy–pressure relationships can be found in Ref. 7.

P–V–T equilibrium phase diagrams

Consider two phases in equilibrium but having different specific volumes v_1 and v_2 respectively. At the equilibrium temperature, the specific Gibbs free energies g_1 and g_2 for each phase can be expressed as a function of pressure from

$$g_1(P+\Delta P) \approx g_1(P) + \left[\frac{\partial g_1(P)}{\partial P}\right]_{\mathrm{T}} \Delta P = g_1(P) + v_1 \Delta P \tag{3}$$

and

$$g_2(P+\Delta P) \approx g_2(P) + \left[\frac{\partial g_2(P)}{\partial P}\right]_{\mathrm{T}} \Delta P = g_2(P) + v_2 \Delta P \tag{4}$$

where ΔP is the pressure increment. These expressions are obtained from the Taylor series truncated after the first derivative. Upon subtracting equation (3) from equation (4) and taking into account the fact that at the equilibrium temperature $g_1(P)=g_2(P)$, we can write

$$g_2(P+\Delta P) - g_1(P+\Delta P) \approx (v_2 - v_1)\Delta P \tag{5}$$

i.e. $g_2 > g_1$ if $v_2 > v_1$.

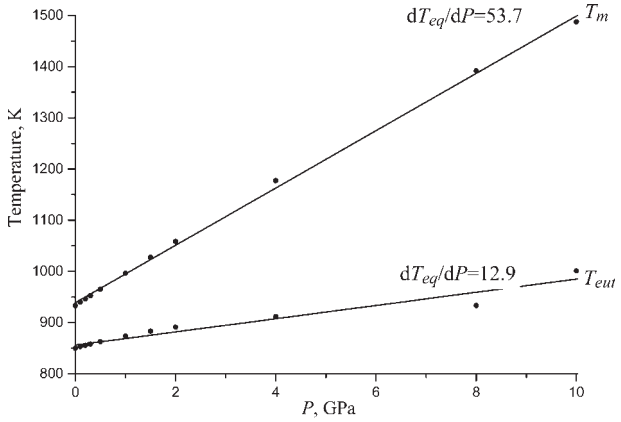

1 Melting point of aluminium T_m and eutectic temperature of Al–Si system T_{eut} as function of pressure

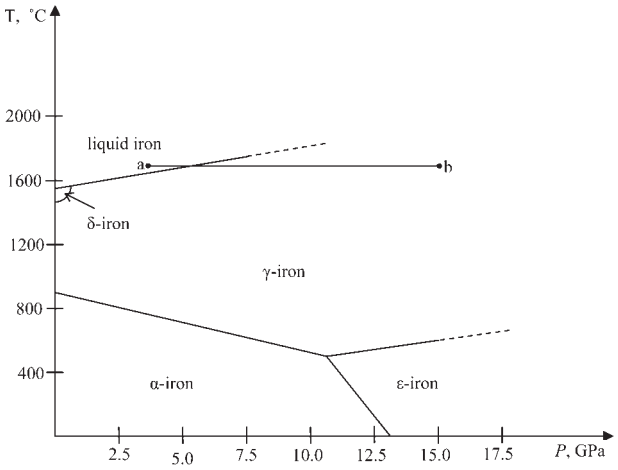

2 *P–T* equilibrium phase diagram for pure iron[8]

This equation suggests that an increase in pressure at constant temperature will shift the equilibrium to the phase of smaller specific volume.

Pressure effects on equilibrium temperature and pressure induced transformations

Phase transformations (melting/solidification, boiling/condensation, sublimation, etc.) in which the specific volumes of the phases are different and involve latent heat are first order transformations. Second order phase transitions do not involve changes in specific volume and latent heat release or absorption. Examples of second order transitions include change from normal liquid ^{4}He to superfluid liquid ^{4}He below 2·2 K, transition from ferromagnetic to paramagnetic behaviour at the Curie temperature, superconductor/normal conductor transition in the absence of magnetic field and others. As this paper is focused on a specific first order transformation, namely, solidification, suffice it to point out that the Ehrenfest equation, given below, describes second order transitions, but their discussion will be excluded from further consideration in the paper

$$\frac{\mathrm{d}T}{\mathrm{d}P}=\frac{Tv(\chi_2-\chi_1)}{c_{\mathrm{P2}}-c_{\mathrm{P1}}} \tag{6}$$

First order phase transformation

First order transitions can be described by the Clausius–Clapeyron equation[7]

$$\frac{\mathrm{d}T}{\mathrm{d}P}=\frac{v_2-v_1}{s_2-s_1}=\frac{T\Delta v}{l_{1\to2}} \tag{7}$$

The equation relates the slope of the temperature–pressure boundary for coexisting phases at some point (T,P) to the specific enthalpy of phase transformation $l_{1\to2}$ and the specific volume change Δv. Equation (7) is very useful because it permits quantitative estimates to be obtained from the thermodynamic parameters for phase transformation. Practical examples of alloy solidification that exhibit the Clausius effect are given in the section on 'Changes in temperature/concentration in equilibrium phase diagrams'.

The Clausius–Clapeyron equation is also written in the equivalent form

$$\frac{\mathrm{d}P}{\mathrm{d}T}=\frac{s_2-s_1}{v_2-v_1}=\frac{l_{1\to2}}{T\Delta v} \tag{8}$$

For solidification, the specific enthalpy for phase change is $l_{1\to2}=Lv_1$

Most metals and alloys expand upon melting so that in equation (7), $\mathrm{d}T/\mathrm{d}P>0$, and a pressure increment will lead to an increase in melting temperature T_{m}. Exceptions include Bi, Sb, Si and hypereutectic cast iron (Fe+C_{gr}), all of which expand upon solidification (i.e. specific volume of solid is greater than specific volume of liquid) so that $\mathrm{d}T/\mathrm{d}P<0$, and pressure increment will decrease the melting point.

Using the Clausius–Clapeyron equation, changes in phase transformation temperature with pressure can be calculated with the formula

$$T_{\mathrm{eq}}(P_0+\Delta P)=T_{\mathrm{eq}}(P_0)+\Delta P\frac{\mathrm{d}T_{\mathrm{eq}}}{\mathrm{d}P}=T_{\mathrm{eq},0}+\Delta P\frac{T_{\mathrm{eq},0}\Delta v}{l_{1\to2}} \tag{9}$$

Figure 1 shows correlations between melting point and pressure for aluminium and the eutectic temperature and pressure for the Al–Si system. These correlations were obtained with ThermoCalc software, and the coefficients $\mathrm{d}T_{\mathrm{eq}}/\mathrm{d}P$ in equation (9) were calculated from the slope. In both cases, the phase transformation temperatures increase with the pressure.

Examples of pressure induced changes in equilibrium states and phase transformations

The pressure induced transformations are shown on the pressure/temperature phase diagram for pure iron (Fig. 2). An increase in pressure depresses the α/γ equilibrium temperature but raises the equilibrium melting temperature. At very high pressures, hcp ε-iron becomes stable. The close packed γ-iron has a smaller specific volume than α-iron. Conversely, because at high pressures ε-iron has a smaller specific volume than γ-iron, pressure increment favours $\gamma\to\varepsilon$ transformation.

In conventional casting practice, solidification occurs due to a decrease in temperature usually at constant pressure. However, crystallisation can also occur by increasing the pressure at a constant temperature, a process called barocrystallisation. Pressure elevation for example causes transformation of the system from state 'a' to state 'b' (Fig. 2). This is not simple solidification under pressure but solidification caused by pressure, and it develops simultaneously in the entire

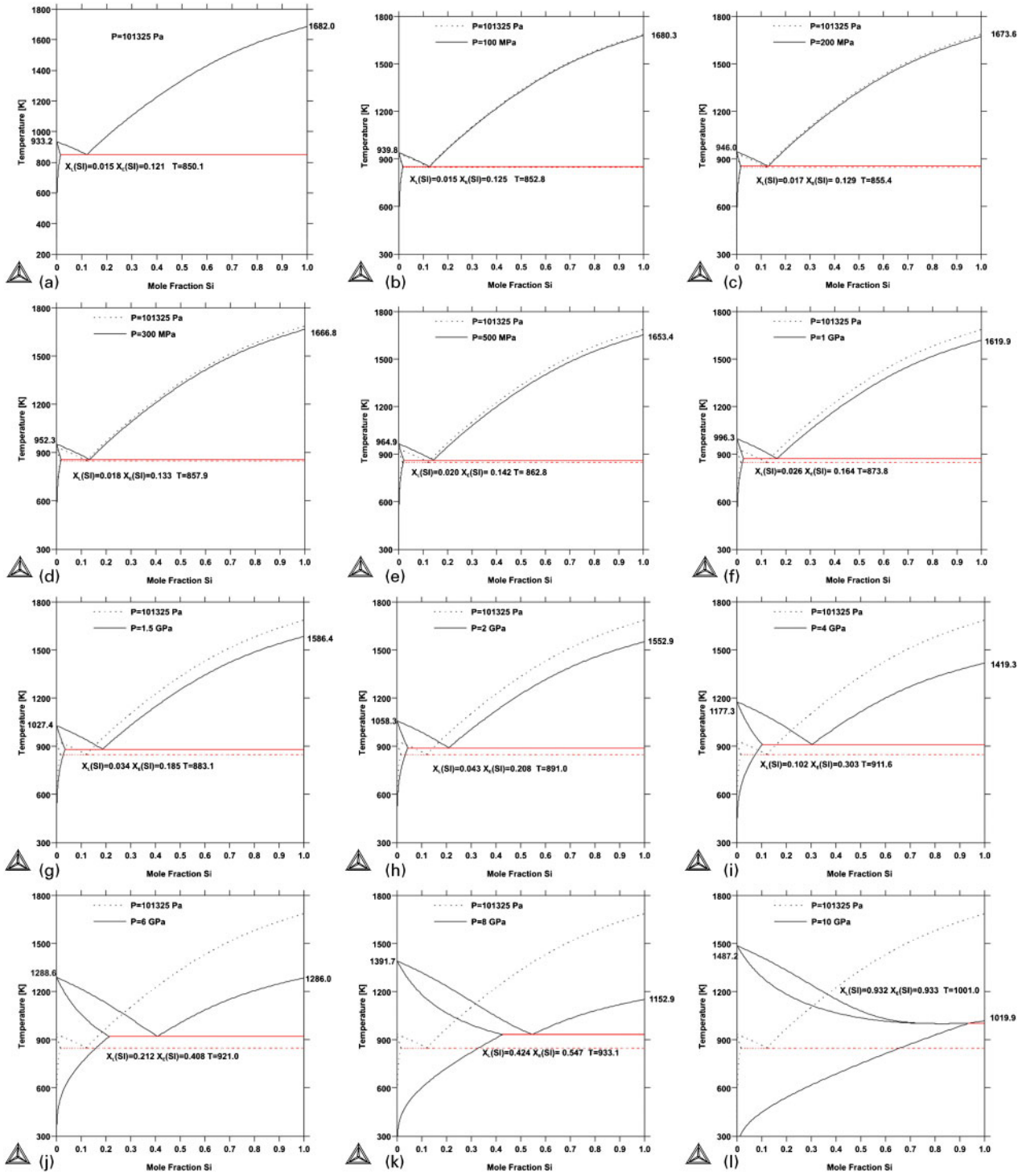

a atmospheric (0·1 MPa); *b* 100 MPa; *c* 200 MPa; *d* 300 MPa; *e* 500 MPa; *f* 1·0 GPa; *g* 1·5 GPa; *h* 2 GPa; *i* 4 GPa; *j* 6 GPa; *k* 8 GPa; *l* 10 GPa

3 Al–Si phase diagram under different external pressures

melt volume. Cooling of the solidified object starts after its solidification. Pressure assisted crystallisation is expected to produce metastable states. If these metastable states possess relatively high activation energy for transition to a more stable state of lower Gibbs free energy, then the metastable state may be found at atmospheric pressure and low temperatures. Pressure assisted crystallisation is a promising technique for obtaining new (not only metallic) materials (e.g. metal–matrix composites) with specific and probably unexpected properties.

Pressure effects on phase diagrams and concentration of alloying elements

Equilibrium phase diagrams strongly depend upon pressure, as demonstrated by the diagrams of the Al–Si system (Fig. 3). These isobaric diagrams are calculated by extrapolation of thermodynamic description from standard conditions[9] to high pressure conditions. The Birch–Murnagham model implemented in ThermoCalc (version P) is used for the calculations. The remaining data necessary to describe high pressure

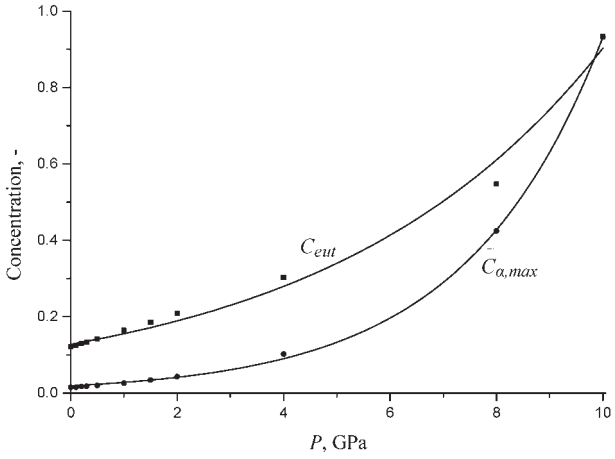

4 Eutectic concentration C_{eut} and maximum concentration in solid solution $C_{\alpha,max}$ of Al–Si system as function of pressure

conditions are taken from Refs. 10 and 11. As the pressure increases, the melting temperature of Al increases but that of Si decreases because Si expands upon solidification.

The equilibrium concentrations of alloying elements also depend upon pressure. The calculated results for eutectic concentration C_{eut} and maximum concentration $C_{\alpha,max}$ of Si in Al in solid solution at eutectic temperature (*see* Fig. 3) are plotted in Fig. 4. The best fitting curve for these data can be expressed in exponential form

$$C_{eq} = C_{eq,0} \exp(bP) \tag{10}$$

The coefficients obtained for C_{eut} are $C_{eut,0}=0{\cdot}128$ and $b=0{\cdot}195$. For $C_{\alpha,max}$, the values are $C_{\alpha,max0}=0{\cdot}019$ and $b=0{\cdot}390$.

The concentration of the alloying elements in α-solid solution of the base metal depends on pressure and cooling rate (the latter is a kinetic effect).[8,12] Because of these effects, phase diagrams can be basically different from equilibrium diagrams. The concentration of alloying elements may increase, decrease or remain constant when the pressure and/or cooling rates increase. This is illustrated in Fig. 5 for an Al base solid solution.

Pressure effects on critical radius for nucleation

Consider a first order phase transformation in which liquid–solid transition with a negative latent heat ($s_2<s_1$, i.e. $l_{1\to2}<0$) and a negative difference of specific volume ($v_2<v_1$) takes place. Here, $dT/dP>0$ in the Clausius–Clapeyron equation (equation (7)). An increase in pressure will increase the melting temperature at a rate of $T\Delta v/l_{1\to2}$, which means

$$T_m(P+\Delta P) > T_m(P) \tag{11}$$

To determine how an increase in melting temperature affects the critical nucleation radius, we consider a melt under pressure P and at temperature T_0 lower than the equilibrium melting temperature T_m^I. At this state (denoted as I), the undercooling is $\Delta T^I = T_m^I - T_0$, and from the classical nucleation theory, the critical nucleus radius is

$$r^{*I} = \frac{2\sigma_{\alpha\beta}}{L\Delta T^I} T_m^I \tag{12}$$

If the pressure increases instantaneously by an amount ΔP, then it will transform the melt into another state (denoted as II) and cause an increase ε of melting temperature $T_m^{II} = T_m^I + \varepsilon$. The undercooling can be expressed as

$$\Delta T^{II} = T_m^{II} - T_0 = T_m^I + \varepsilon - T_0 = \Delta T^I + \varepsilon \tag{13}$$

and the critical radius will be

$$r^{*II} = \frac{2\sigma_{\alpha\beta}}{L\Delta T^{II}} T_m^{II} \tag{14}$$

Upon substituting equation (13) in equation (14) and following simple transformation, equation (14) becomes

$$r^{*II} = \frac{2\sigma_{\alpha\beta}}{L(\Delta T^I + \varepsilon)} T_m^I + \frac{2\sigma_{\alpha\beta}}{L(\Delta T^I + \varepsilon)} \varepsilon \tag{15}$$

For all cases involving metals and alloys, $\varepsilon << T_m^I$; therefore, the second term in equation (15) can be neglected, and equation (15) can be written as

$$r^{*II} = \frac{2\sigma_{\alpha\beta}}{L(\Delta T^I + \varepsilon)} T_m^I \tag{16}$$

Using equations (12) and (16), it can be shown that

$$\frac{r^{*I}}{r^{*II}} = 1 + \frac{\varepsilon}{\Delta T^I} > 1 \tag{17}$$

Equation (17) shows that the pressure increase will decrease the critical radius for nucleation, which in turn will increase the number of nuclei per unit volume. Thus, for solidification with negative latent heat and with specific volume of solid less than that of liquid, an increase in pressure will refine the solid's structure. In addition to its effect on nucleation, pressure effects manifest themselves at the macrolevel, which further promotes structure refinement, as discussed later.

Following the same procedure, it can be shown that when solidification is accompanied by negative latent heat and a positive difference in specific volume ($v_2>v_1$) as in the freezing of water, the pressure increase will coarsen the solid structure because $r^{*I} < r^{*II}$.

Pressure effect on interfacial free energy

Generally, phase transformations in metals (in solid, liquid or vapour state) occur by the nucleation and growth of new phases from a few nucleation sites within the parent phase. The great majority of physical processes are directly connected with the creation of interfaces and associated interfacial free energy. The free energy of the system containing an interface of area A and the interfacial free energy per unit area σ are related from

$$G = G^0 + A\sigma \tag{18}$$

where G^0 is the free energy of the system assuming there are no interfacial effects and $A\sigma$ is the excess free energy arising in the system because some material lies in or close to the interface. Consider an interface γ between two homogeneous phases, solid α and liquid β (Fig. 6).[7] The interface is displaced, as on a solidification front where growing crystals contact the melt. Assume that the boundaries α/γ and β/γ are planes parallel to each other. Close to the boundary α/γ, the properties are identical with those of the phase α, and close to the boundary β/γ, they are identical with those of the phase β. The thickness of the interface region γ is usually

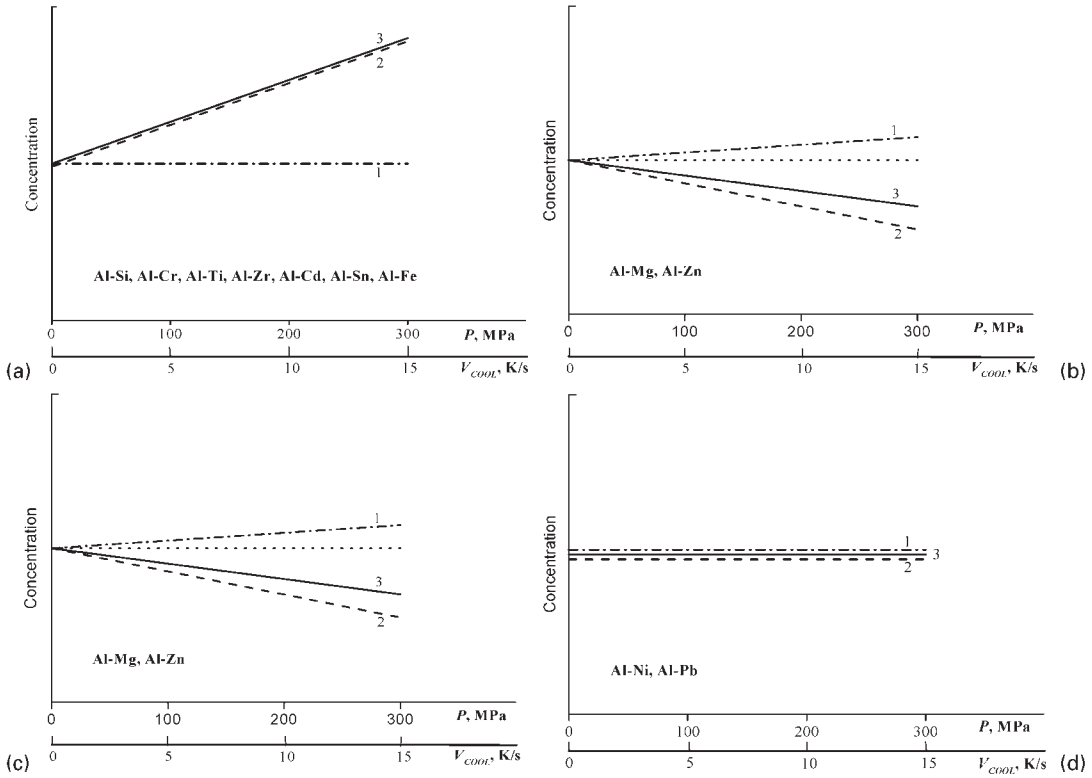

a systems Al–Si, Al–Cr, Al–Ti, Al–Zr, Al–Cd, Al–Sn and Al–Fe; *b* systems Al–Mg and Al–Zn; *c* systems Al–Cu and Al–Mn; *d* systems Al–Ni and Al–Pb

5 Schematic representation of effect of (1) cooling rate V_{cool} and (2) pressure P and (3) their combined effect on crystallisation under pressure C_{P+V} in aluminium based solid solution: based on analysis of experimental data of Refs. 13 and 14

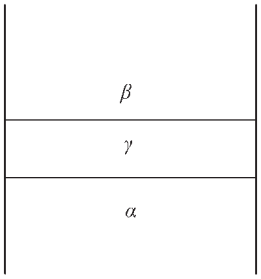

6 Schematic presentation of interface between two homogeneous phases

between 10^{-8} and 10^{-9} m or even less, i.e. only a few atomic layers.

Writing equation (18) in terms of Gibbs free energies per unit area of the interface G_A ($=G/A$) and G_A^0 ($=G^0/A$), and differentiating the resulting equation with respect to P at constant temperature, we obtain

$$\left(\frac{\partial G_A}{\partial P}\right)_T = \left(\frac{\partial G_A^0}{\partial P}\right)_T + \left(\frac{\partial \sigma}{\partial P}\right)_T \tag{19}$$

Noting from equation (2) that $(\partial G/\partial P)_T = V$, equation (19) can be written as

$$V_A = V_A^0 + \left(\frac{\partial \sigma}{\partial P}\right)_T \tag{20}$$

Here, $V_A = V/A$ and $V_A^0 = V^0/A$ are volumes of the system per unit area of the interface. On the other hand, the volume of the system is a function of T and P, and for constant temperature, V_A can be expressed by the first two terms of the Taylor series in the form of

$$V_A = V_A^0 + \Delta P\left(\frac{\partial V_A}{\partial P}\right)_T \tag{21}$$

Combining equations (20) and (21) yields the relation

$$\left(\frac{\partial \sigma}{\partial P}\right)_T = \Delta P\left(\frac{\partial V_A}{\partial P}\right)_T \tag{22}$$

Equation (22) describes the effect of pressure on the interfacial free energy. As the volume of every closed system with constant phase composition decreases with pressure, i.e. $(\partial V_A/\partial P)_T < 0$, an increase in pressure will decrease the interfacial free energy.

For liquids, a surface with free energy σ (J m^{-2}) exerts a surface tension σ (N m^{-1}). This is not strictly true for solids because of the very low (relative to liquids) atomic mobility in solids. Only at temperatures close to melting point do the atomic mobilities in liquid and solid become commensurate, and the interfacial free energy and surface tension can be considered as identical quantities for the solid.

The interfacial free energy determines the critical radius for solid phase nucleation (equation (2)). Since an increase in pressure decreases the interfacial free energy (surface tension) of the crystal/melt interface, the critical radius for nucleation will decrease proportionally. This in turn will increase the number of nucleation sites and consequently refine the solidified structure. It is well known that application of high pressures improves the wettability of phases that normally do not wet each other.[15] Squeeze casting makes use of this fact to produce a wide variety of metal–matrix composites and fine grained alloy castings with superior properties.

Pressure effect on chemical potential, entropy, enthalpy and heat capacity

The isothermal compressibility k_T of solids and liquids, except near the critical temperature, only marginally depends on the pressure. Because of this, it can be shown,[7] without any essential loss of accuracy, that

$$-V^{-1}\left(\frac{\partial V}{\partial P}\right)_T = k_T = \text{constant} \tag{23}$$

Integrating this expression at constant temperature yields

$$V_m = V_m^0 \exp[-k_T(P-P_0)] \tag{24}$$

where V_m^0 is the value of V_m at pressure P_0 for example at 1 atm pressure.

For most liquids and solids, k_T is not greater than 10^{-9} Pa^{-1}. Therefore, equation (24) can be replaced by

$$V_m = V_m^0[1-k_T(P-P_0)] \tag{25}$$

Integrating equation (25) at constant temperature and noting [from equation (2)] that $(\partial G/\partial P)_T = V$, we obtain for the chemical potential of a one-component system

$$\mu = \mu_0 + V_m^0\left[(P-P_0) - 0{\cdot}5k_T(P-P_0)^2\right] \tag{26}$$

This can be transformed to a more compact form

$$\mu = \mu_0 + 0{\cdot}5(P-P_0)\left(V_m + V_m^0\right) \tag{27}$$

Equation (27) expresses the dependence of the chemical potential of a one-component system on pressure at constant temperature. Upon differentiating equation (27) with respect to T at constant pressure, we obtain the following relationship between specific entropy and pressure

$$\begin{aligned} S_m &= -\left(\frac{\partial \mu_0}{\partial T}\right)_P - 0.5(P-P_0)\left(\chi V_m + \chi_0 V_m^0\right) \\ &= S_m^0 - 0.5(P-P_0)\left(\chi V_m + \chi_0 V_m^0\right) \end{aligned} \tag{28}$$

where χ and χ_0 are the coefficients of thermal expansion at pressures P and P_0 respectively, and S_m^0 is the specific entropy at pressure P_0. Finally, from equations (27) and (28), we obtain the following relationships for specific enthalpy and specific heat capacity as a function of pressure

$$\begin{aligned} S_m = \mu + TS_m &= \mu_0 - T\left(\frac{\partial \mu_0}{\partial T}\right)_P + \\ &0.5(P-P_0)\left[V_m(1-\chi T) + V_m^0(1-\chi_0 T)\right] \end{aligned} \tag{29}$$

$$\begin{aligned} C_P^0 = &-T\left(\frac{\partial^2 \mu_0}{\partial T^2}\right)_P - \\ &0.5(P-P_0)T\left[V_m\left(\frac{\partial \chi}{\partial T}\right)_P + V_m^0\left(\frac{\partial \chi_0}{\partial T}\right)_T\right] \end{aligned} \tag{30}$$

Both formulae express the enthalpy and heat capacity as linear functions of applied pressure.

Kinetics

Pressure effect on nucleation rate

The classical theory of nucleation gives the nucleation rate as a function of the activation free energy barrier for phase transformation and the free energy change related to a nucleus with critical radius. The nucleation rate is expressed as[8]

$$N = N_S \frac{k_b T}{h}\exp\left(-\frac{\Delta G_m}{k_b T}\right)\exp\left(-\frac{4\pi\sigma_{\alpha\beta}}{3k_b T}S_f r^{*2}\right) \tag{31}$$

Equation (31) shows that the nucleation rate increases exponentially if the critical radius decreases, which is the case for transformations with negative latent heat and $v_2 < v_1$. For the case with $v_2 > v_1$, the nucleation rate will decrease rapidly with an increase in pressure. Thus, the pressure increment will cause substantial changes to both the number of nuclei per unit volume and the nucleation rate. This combined effect shows the important role the application of pressure could play in structure formation.

From equation (31), the ratio of nucleation rates at pressures P_0 and P (with $P > P_0$) is

$$\begin{aligned} \frac{N(P)}{N(P_0)} = &\exp\left[\frac{\Delta G_m(P_0) - \Delta G_m(P)}{k_b T}\right] \\ &\exp\left[A\sigma_{\alpha\beta}(P_0)r^{*2}(P_0) - A\sigma_{\alpha\beta}(P)r^{*2}(P)\right] \end{aligned} \tag{32}$$

where $A = (4\pi S_f/3K_b T)$, and $\Delta G_m(P_0)$ and $\Delta G_m(P)$ denote the values of ΔG_m at pressures P_0 and P respectively, $\sigma_{\alpha\beta}(P_0)$ and $\sigma_{\alpha\beta}(P)$ are the interfacial free energies at pressures P_0 and P respectively, and $r^*(P_0)$ and $r^*(P)$ are the critical radii of the nuclei at pressures P_0 and P respectively. In most alloy systems, $\Delta G_m(P) < \Delta G_m(P_0)$. Furthermore, since an increase in pressure decreases the interfacial free energy of the crystal/melt interface, the critical radius for nucleation will decrease in the same degree (see the section on 'Pressure effect on interfacial free energy'). Equation (32) shows that both of these factors contribute to a significant (exponential) increase in the nucleation rate during solidification under high pressure. This indicates that there would be more nuclei and less space for the growth of the nuclei under pressure than in conventional solidification. As the activation energy for crystal growth mainly depends on the activation energy for diffusion and as for most alloy systems, the pressure increases the activation energy for diffusion, and for crystal growth, pressure application can accelerate nucleation and restrain growth during solidification, thereby refining the grain structure.

In the case of multicomponent solutions or alloys, the role played by solutes in nucleation must be considered. Pressure effects on nucleation rate in solutions have been theoretically examined by Kashchiev and van Rosmalen,[16] who presented a general theory for the effect of pressure on the nucleation rate of solid or liquid phases in solid or liquid solutions at different pressures. They found that high pressures inhibited or stimulated the nucleation process when the partial molar volume of solute was respectively larger or smaller in the nucleating phase than in the solution. Other theoretical studies[17] have examined the effect of pressure on the formation of non-spherical nuclei during phase change.

Experimental studies on the effect of pressure on the nucleation rate during metal solidification are scant. However, pressure effects on nucleation have been experimentally studied in gas–liquid systems as well as in liquid solutions. Huang[18] studied the pressure effects on the nucleation and growth of polycrystalline quartz

formed from amorphous silica in water at 50–450°C temperature and 50 MPa to 3 GPa pressure. At low 100–200 MPa pressures, the experimental results could be modelled using Avrami's nucleation and growth equation.[8] At higher pressures, experiments revealed a dramatic effect of pressure on the transformation rate, which increased approximately by five orders of magnitude as the pressure increased from 50 MPa to 3 GPa.[18] The authors noted that pressure could significantly enhance both nucleation and growth rates, although the effect was stronger on nucleation than on growth. The SEM observations showed that the grain sizes decreased significantly with increasing pressure, which is consistent with similar observations on metal solidification.

In the case of gas–liquid systems, the influence of pressure of a carrier gas on the nucleation rate has been studied.[19] The results show that the effect can be positive, negative or neutral. In fact, the same experiment may show positive and negative trends for the same substance, depending on temperature, or for different substances at the same temperature. The ambiguity is believed to arise from a competition between non-isothermal effects and pressure–volume work, and its existence has been corroborated by molecular dynamics (MD) simulations.[19] Research in nanotechnology and developments in increasingly sophisticated analytical instrumentation present a new opportunity to resolve such ambiguities in nucleation under pressure.

Pressure effect on diffusion coefficients

Thermodynamically, the driving force for diffusion is the lowering of Gibbs free energy. Diffusion in solids occurs either via the lattice or via structural defects, such as along dislocation cores, interfaces, grain boundaries and free surfaces. Phenomenologically, diffusion obeys Fick's laws, and the diffusion coefficient is expressed by an Arrhenius type equation[8]

$$D = B\exp\left(-\frac{\Delta G_{\mathrm{m}}}{k_{\mathrm{b}}T}\right) \tag{33}$$

where B is the frequency factor or pre-exponential term and is independent of temperature. Equation (33) is valid for all types of solid state diffusion processes, which formally differ only in the numerical value of B and the activation energy ΔG_{m}. The activation energy depends on pressure and for small pressure increment at constant temperature

$$\Delta G_{\mathrm{m}}(P_0+\Delta P) = \Delta G_{\mathrm{m}}(P_0) + \left(\frac{\partial \Delta G_{\mathrm{m}}}{\partial P}\right)_{\mathrm{T}} \Delta P \tag{34}$$

It has been found[12] that for most cases of practical interest, the activation energy increases with increasing pressure according to

$$\Delta G_{\mathrm{m}}(P) = \Delta G_{\mathrm{m}}(P_0)(1+aP) \tag{35}$$

Upon differentiating equation (35), we obtain

$$\left(\frac{\partial \Delta G_{\mathrm{m}}}{\partial P}\right)_{\mathrm{T}} = a\Delta G_{\mathrm{m}}(P_0) = A \tag{36}$$

Here, A does not depend on pressure. Using equation (36), equation (34) transforms to

$$\Delta G_{\mathrm{m}}(P_0+\Delta P) = \Delta G_{\mathrm{m}}(P_0) + A\Delta P \tag{37}$$

Following the substitution of equation (37) in equation (33), we obtain

$$\begin{aligned} D(P_0+\Delta P) &= A\exp\left[-\frac{\Delta G_{\mathrm{m}}(P_0)}{k_{\mathrm{b}}T}\right]\exp\left(-\frac{A\Delta P}{k_{\mathrm{b}}T}\right) \\ &= D_0\exp\left(-\frac{A\Delta P}{k_{\mathrm{b}}T}\right) \end{aligned} \tag{38}$$

Here, $D_0 = B\ \exp\langle -\{[\Delta G_{\mathrm{m}}(P_0)]/k_{\mathrm{b}}T\}\rangle$ is the diffusion coefficient at pressure P_0. Equation (38) shows that when the pressure in a system increases by an amount ΔP, the diffusion coefficient decreases exponentially. A low value of the diffusion coefficient diminishes the velocity of redistribution of the alloying elements during phase transformation (e.g. solidification), which affects the degree of chemical homogenisation into crystals formed. This explains why thermal processing for homogenisation of the composition is facilitated at low pressures. The effect of pressure on the diffusion coefficient can be demonstrated by the solidification of Al–4·5Cu alloy under different pressures. A rise in pressure from 50 to 200 MPa causes an increase in Cu content in the central zone of the dendritic cells from 1·0 to 1·9%.[12] While such studies provide indirect proof for the effect of pressure on diffusion, direct proof for pressure effects on diffusion comes from the measurement of the diffusion coefficient in the solid state. In fact, pressure effects on the diffusion coefficient have been extensively studied for metals[20–24] and include studies on self-diffusion in Ge[23] and Si[24] and on diffusion of arsenic in germanium.[25] The diffusivity of arsenic in germanium for example is enhanced[25] under high pressures (0·1–4 GPa). High pressures can either increase or decrease the diffusion, depending upon the operating diffusion mechanism. If the mechanism involves interstitial diffusion, then high pressures will inhibit the diffusion. For substitutional diffusion, the effect of pressure will depend on the size of the substitutional atom.

Practical aspects of high pressure liquid phase processing

Many of the pressure effects on the thermodynamic and kinetic parameters become significant and measurable at pressures that are far in excess of those that can be achieved using conventional equipment. Such limitations notwithstanding, some of the effects of pressure have been revealed in studies on alloy solidification under moderate levels of pressure. Our goal in this section is to present observations of pressure effects in practical alloy systems and rationalise the observations within the theoretical framework of the preceding sections. Clearly, efforts to achieve greater pressures must be made in concert with the effort to improve the sensitivity of instruments designed to measure the pressure effects on thermodynamic and kinetic parameters.

Casting techniques that utilise gas pressure are the counter pressure casting method,[26] autoclave casting, low pressure permanent mould casting and vacuum permanent mould casting (the latter technique utilises negative pressure for controlled flow). In all these techniques, the magnitude of pressure does not reach extremely high values, but these methods allow flexible

control of form filling, feeding of shrinkage, cooling conditions (especially counter pressure casting method) and improved final structure of the cast product.

Mechanical means to apply larger pressures are used in squeeze casting,[12] in which specially designed pistons permit realisation of high pressure during solidification. The method shortens production cycle, provides better structure and is applicable to both cast and wrought metals and alloys and their composites. In squeeze cast metal–matrix composites, high pressures not only eliminate porosity and facilitate capillary penetration of fibre preforms but also improve the fibre/matrix wetting and bonding[27–29] and thereby the load bearing capacity of the composite. Improved mechanical properties and resistance to thermal fatigue and corrosion are some of the advantages of squeeze cast parts.[30,31] Since pressure improves the bonding of chemical phases present in a substance, it also affects the electrical and magnetic properties of the material. The microstructural refinement, integrity and improved physical and mechanical properties of squeeze cast products are desirable for many critical applications.

Phenomena at macroscale

Heat transfer between casting and mould

Owing to the plasticity of metal slurry and the solid close to solidus temperature, an increase in pressure during the solidification of castings improves the thermal contact between the casting and the mould. External pressure during solidification improves the metal/die contact and raises the heat transfer coefficient.[32] Theoretical and experimental studies[33] on the solidification of Al–Si eutectic alloy against steel dies have shown that a pressure of 196 MPa increased the heat transfer coefficient h by a factor of 15 from about $3{\cdot}4\times10^3$ to $5{\cdot}25\times10^4$ W m^{-2} K^{-1}. Such an increase in h intensifies heat removal from the casting,[34,35] which increases the cooling rate and the temperature gradient in the casting and increases the melt undercooling ΔT.

The critical radius for solid phase nucleation decreases linearly with ΔT, but the free energy for nucleation decreases as $1/(\Delta T)^2$. The rate of nucleation increases faster because the free energy term is in the exponent. This means that the casting solidification will be facilitated by copious nucleation, and as a result, the cast structure will develop from finer grains. It is necessary to recall that pressure affects also the temperature for equilibrium phase transformation and surface tension. To be precise, the real values of ΔT, T_{m} and $\sigma_{\alpha\beta}$ could be used for each particular case. Practical consequences of grain size reduction are an increase in microhardness, mechanical strength and corrosion resistance of the cast material.

Depression or elimination of shrinkage defect

Pressure applied to solidifying casting depresses and could even eliminate the shrinkage defect. The reason is that pressure 'injects' melt into the interdendrite space and into the shrinkage microcavities formed during solidification and in this way eliminates the defect. Thus, liquid movement under pressure can produce virtually pore-free casting.[36] Pressure risering in skin forming alloys is a typical example of how atmospheric pressure acts to feed the shrinkage when the hermetic solidified skin is punctured. Likewise, self-feeding is typical for casting techniques, which apply elevated pressures such as squeeze casting. Therefore, for casting under high pressure, there is no need to design feeders because the pressure facilitates self-feeding. Pressure induced interdendritic flow can also produce segregation in castings.

Both shrinkage formation and externally applied pressure during solidification modulate the shape of the two-phase region in the casting and generate mass flow into this region. Thus, some dendrites are destroyed, and the broken fragments are transported to other areas, where they act as nucleation sites for crystal formation; this further increases the nucleation rate and refines the cast structure. This effect is more pronounced for melt compositions of large freezing range alloys with a wide two-phase (mushy) zone in their phase diagram.

Increase in gas solubility

Sievert's law relates gas concentration in a substance, its temperature and gas pressure above the substance. This law is written as

$$\ln C = -\frac{A}{T} + B + 0{\cdot}5\ln P \tag{39}$$

According to Sievert's law, the higher the pressure, the larger the amount of dissolved gas. If a melt is prepared under pressure P_1 and solidifies under an elevated pressure P_2 ($P_1<P_2$), then the gas evolution in solid will be depressed. There is a threshold pressure specific for each metal/gas system above which the entire amount of gas will remain in the solid in atomic form, i.e. gas porosity will not occur. The combined effect of this phenomenon and the melt injection prevents gas porosity and shrinkage cavity from developing in casting.[37] Additionally, processing of metallic melts under high gas pressure is also an effective way to introduce certain gaseous substances as alloying elements (e.g. nitrogen steels).

Phenomena at microscale

Changes in temperature/concentration in equilibrium phase diagrams

The application of pressure not only alters the transformation temperature but also generates new phases or causes some phases to disappear. The case of disappearance of a phase and the appearance of other phases caused by pressure increase can be observed in Fig. 2 for iron. The δ phase exists only at relatively low pressures, and the ε phase appears under high pressures. Such effects can be readily visualised with the help of three-dimensional phase diagrams that reveal phases as a function of temperature, concentration and pressure. Different cross-sections of these diagrams at fixed values of concentration or pressure give simpler representation of the regions of interest.

Changes in the equilibrium melting temperature due to static pressure changes (Claperyon effect) can significantly influence crystal growth[38] and permit not only reliable estimates of volumetric changes upon solidification to be made but also management of crystal growth. If $\Delta V_{\mathrm{m}}<0$, which is the case with Sb, Bi and also water, then the melting temperature will decrease when the pressure is increased. For example, the melting temperature of ice at atmospheric pressure (0·1 MPa) is close to 0°C, but under 200 MPa pressure, the melting temperature of ice decreases to −32°C.[39] For pure

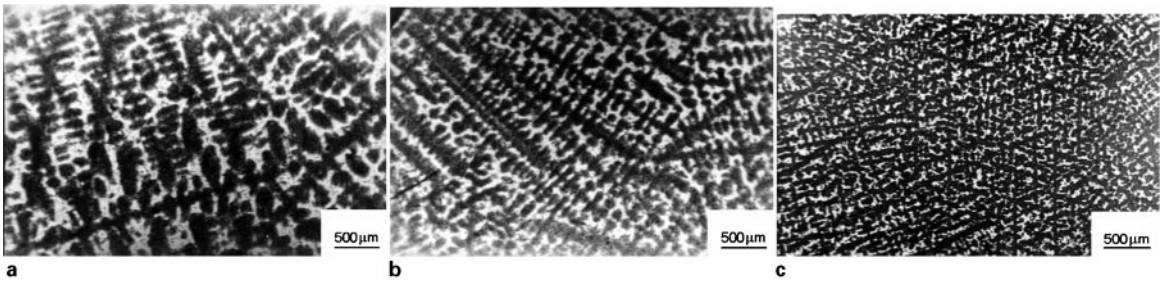

a LST=725 s, V_{cool}=0·17°C s^{-1}, P_1=0·1 MPa; *b* LST=418 s, V_{cool}=0·3°C s^{-1}, P_2=1·7 MPa; *c* LST=60 s, V_{cool}=2·0°C s^{-1}, P_3=3·6 MPa

7 Structure of high nitrogen steel solidified in metal mould under different gas pressures:[41] all structures are observed in very same region of ingots

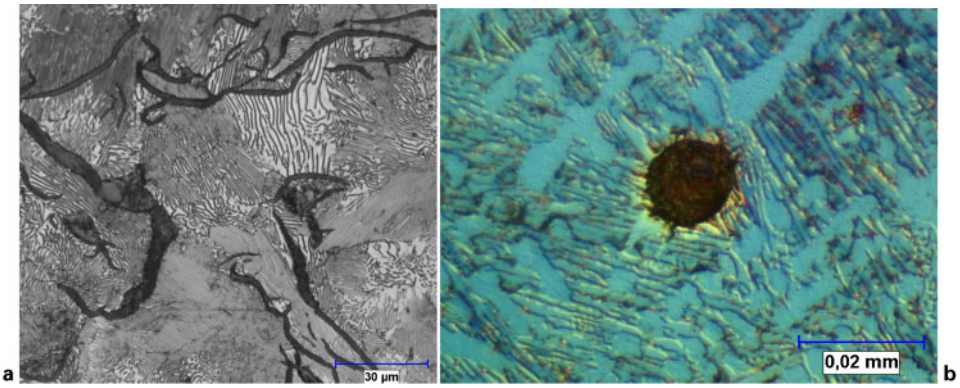

a structure of cast iron formed under atmospheric pressure; *b* structure formed after remelting under pressure of 4·3 MPa and containing spheroidal graphite particles

8 Spheroidisation of graphite particles induced by high pressure

aluminium, the situation is opposite because $\Delta V_m > 0$ and the melting temperature increases from 660°C at atmospheric pressure up to 940°C under 500 GPa pressure.[12] This is because high pressures favour the formation of phases with lower specific volume.

High melting temperatures are associated with high values of dT/dP in the Clausius equation. Consequently, under high pressures, the melting temperature of metals increases to different absolute values. This in turn affects the undercooling during solidification and the structure and properties of the cast product.

Solidification under pressure offers evidence of an interesting temperature–memory effect.[40] The situation is as follows. Consider three solid Zn samples solidified under different pressures. The first sample was solidified under 200 MPa pressure, the second one was solidified under 2000 MPa pressure and the third one was solidified under atmospheric pressure. These samples were then remelted under atmospheric pressure. It was found[40] that the first sample had a melting temperature of 3°C higher than the third one, and the second sample had a melting temperature of 6°C higher than the third one. This is evidence of a kind of 'historically' determined effect. Such an increase in melting temperature has also been observed in Sn and Cd. However, unlike Zn, Sn and Cd, in the case of Bi, there is a measurable decrease rather than an increase in melting temperature. These results show that the metal has a memory of the temperature change, which has been shown to be linked to the resistance to the motion of dislocations in metal lattices under high pressure.[40]

Some particular results related to pressure effect utilisation

There are some important transformations in casting structure formation that appear even at relatively small increases of pressure. An example is given in Fig. 7. The structures shown are formed in high nitrogen steel ingots solidified in a metal mould under various gas pressures: P_1=0·1 MPa, P_2=1·7 MPa and P_3=3·6 MPa. Owing to the plasticity of semisolid and solid regions of solidifying ingot, the heat exchange between mould and casting is forced by an external pressure, which results in a reduction in total solidification time, decrease in local solidification time (LST), increase in cooling rate V_{cool} and, finally, refinement of the dendritic structure.

Another significant example related to the pressure effect on the structure formed in liquid phase processing is shown in Fig. 8. Grey silicon cast iron (3·80C–1·70Si–0·27Mn–0·02P–0·02S, according to EN-GJS-500-15) solidified under atmospheric pressure was remelted in a levitation experiment under a relatively high argon gas pressure of 4·3 MPa. Rapid solidification under these conditions led to the spheroidisation of the graphite particles.

Extensive research has been performed on phase transformation, new phase formation and grain refinement in cast products caused by high external pressures. Aluminium, magnesium and lead alloys have been solidified under pressure and examined for physical, structural and chemical changes.[42–46] Thus, solidification of Al–20 wt-%Mn alloy under pressures of up to 6 GPa[42] led to a new Al–Mn phase with needle-like morphology and Al nanocrystallites of size <20 nm.

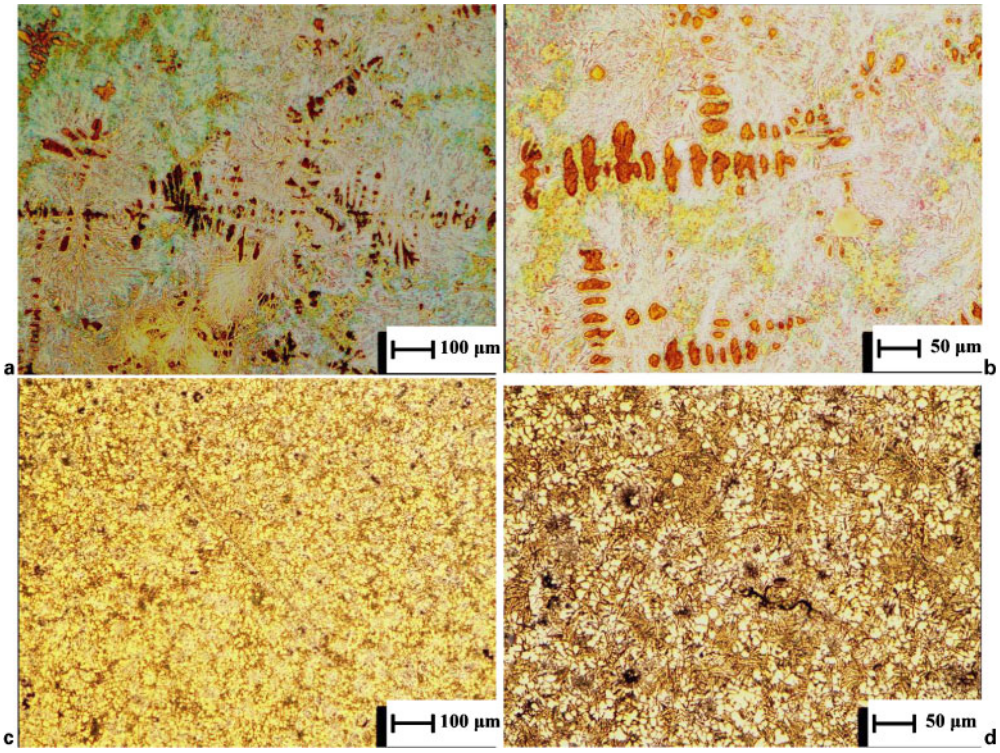

9 Light microscopy images of 413·0 Al alloy solidified under *a*, *b* atmospheric pressure and *c*, *d* pressure of 34 MPa

The new phase had a composition of $Al_{77·5}Mn_{22·5}$ and consisted of C centre orthorhombic unit cell with lattice constants of a=0·7565(4) nm, b=1·2965(6) nm and c=0·7801(6) nm. Similarly, high density bulk nanocrystalline (NC) Pb–Sn–Te alloys have been prepared by quenching the melt under high pressures.[43] Enhanced nucleation and restricted growth under pressure led to NC grains (mean size of ~100 nm), improved thermoelectric properties, clean crystalline interfaces and homogeneous grain size.

The effect of pressure on the grain size of an NC Fe–Mo–Si–B alloy was studied by annealing amorphous $(Fe_{0·99},Mo_{0·01})_{78}Si_9B_{13}$ alloy in the temperature interval from 723 to 933 K and pressure of 3–6 GPa.[44] It was established that the average grain size decreased from 43 nm at 3 MPa pressure to 25 nm at 6 MPa pressure because high pressures increased the nucleation rate.

Grain refinement at the nanometre scale under pressure has also been reported in $Mg_{65}Cu_{25}Y_{10}$ alloy.[45] Under ambient pressures, molten $Mg_{65}Cu_{25}Y_{10}$ alloy solidified polymorphously into $Mg_2(Cu,Y)$ and a small amount of Y_2O_3 inclusions. Under 2 GPa pressure, a new phase $Cu_2(Y, Mg)$ emerged. With an increase in pressure from 2 to 5 GPa, the average grain sizes of $Mg_2(Cu,Y)$ and $Cu_2(Y,Mg)$ decreased from the 125–96 nm range to the 80–7 nm range. As the undercooling of $Cu_2(Y,Mg)$ was much larger than that of $Mg_2(Cu,Y)$,[45] the application of pressure caused the formation of nanometre sized $Cu_2(Y,Mg)$.

The effect of pressure application on the microstructure of a 413·0 Al–Si alloy [nominal composition: 12·90Si, 0·82Fe, 0·04Cu, 0·20Mn, 0·01Mg, 0·006Ni, 0·03Zn, 0·02Pb, 0·008Ti, 0·013Cr, 0·023 other (wt-%)] is shown in Fig. 9.[46] This figure compares the microstructures obtained in a cast product solidified at a pressure of 0·1 MPa (atmospheric pressure) (Fig. 9*a* and *b*) and another cast product solidified under a pressure of 34 MPa (Fig. 9*c* and *d*). A notable refinement of the obtained structures was achieved (Fig. 9*c* and *d*). The amount of Al rich α-phase also increased from 21·87 vol.-% at 0·1 MPa to 46·23 vol.-% at 34 MPa pressure. An increase in the eutectic concentration of ~20 wt-% higher in Si content in the Al–Si phase diagram was noted. The applied pressure also increased the eutectic temperature by 5°C. Thus, higher pressures stimulate refinement of the microstructure together with a shift of the eutectic point towards higher Si contents, which makes the alloy hypereutectic. Information about similar effects on other squeeze cast Al–Si alloys can be found in Ref. 12. Aluminium and its alloys are the most commonly squeeze cast alloys because they have relatively large two-phase (mushy) zones in their equilibrium diagrams, and shrinkage effects during solidification cannot be neglected.

For most metals and alloys, the high pressures applied during solidification decrease the grain size, but this is not valid for all cases. The Clausius–Clapeyron effect determines changes in temperature and grain size associated with a certain phase transformation. An example of reduction in solidification temperature and increase in grain size caused by higher pressure can be found in Ref. 47. The authors developed a technique for the crystallisation of thin films from pyrochlore $Pb_2Nb_2O_7$ at low temperatures and high pressures. Under rapid thermal annealing at atmospheric pressure, recrystallisation of amorphous $Pb_2Nb_2O_7$ was realised at the temperature of 600°C. The structure of the obtained film consisted of small grains of about 20–30 nm in size when recrystallisation occurred under 2–8 MPa pressure.

Pressure induced phase transitions from graphite eutectic to carbide eutectic have been observed[48] in Fe–3%C–4%Si alloys. Solidification under large (~800 MPa) pressures led to the formation of a carbide eutectic

observed in the inner region of the specimens. The observed transitions from graphite eutectic to carbide eutectic were explained by the pressure dependence of the stable and metastable eutectic temperatures.

It is pertinent to parenthetically remark here that large pressures have also been profitably used in high temperature processes (e.g. sintering and pyrolysis) other than solidification. Bulk C_3N_4 for example has been prepared through high pressure pyrolysis of melamine ($C_3N_6H_6$) at different temperatures.[49] The route elaborated is considered as novel for the synthesis of theoretically superhard cubic C_3N_4 and other C_3N_4 phases from organic compounds using high pressures and high temperatures. Another superhard material MgB_2 has been synthesised by sintering under high pressure (5·5 GPa) and high temperatures.[50] Under similar conditions in the Pb–Te system, lead telluride (PbTe) with rock–salt structure was obtained.[51]

Pressure effects of ultrasonic irradiation

The effects of vibration on solidification have been discussed in depth by Campbell.[52] The local pressure fluctuations caused in a solidifying melt by propagating ultrasonic waves induce cavitation (nucleation and collapse of tiny gas filled microcavities or bubbles).[53–57] When ultrasound is introduced into molten metals, the local increase in pressure and temperature due to cavitation can be expressed from[53]

$$P = P_0 \left[\frac{P_m(\gamma - 1)}{P_0} \right]^{\gamma/\gamma - 1} \tag{40}$$

$$T = T_0 \left[\frac{P_m(\gamma - 1)}{P_0} \right] \tag{41}$$

where P_m is the pressure amplitude of the ultrasonic wave, P_0 is the hydrostatic pressure, T_0 is the temperature of the melt, γ is the specific heat ratio (polytropic index of gas in the bubble) and P and T are the pressure and the temperature of the melt due to ultrasonic treatment. Using typical values for the Al melt, equations (40) and (41) yield $P \approx 6$–7 GPa and $T \approx 10^4$ K respectively.[57] The large local pressures will desorb surface impurities, and the increased temperatures due to cavitation will improve the wettability. Additionally, nucleation of crystals is enhanced when the solidifying melt is irradiated with ultrasound. The nucleation density in the presence of ultrasound can be calculated by combining equations (40) and (41) with the Clausius–Clapeyron equation and the nucleation equation $n = A(\Delta T)^2$. This allows for the effect of pressure change on the depression of solidification temperature ΔT_f to be estimated. It is found[54] that with an increase in ultrasonic power, the nucleation density increases, and the solidification structure is refined. Normally, it is somewhat difficult to significantly modify the solidification microstructure by application of pressure because of the small melting temperature/pressure coefficient (typically $\sim 0{\cdot}01$ K atm^{-1}). However, formation and collapse of bubbles due to cavitation in solidifying metals can locally generate enormous pressures that could alter the phase change temperature by dozens of degrees.

Experiments[52] have shown that solid could be nucleated by bubble collapse in an undercooled liquid regardless of whether the solidification was accompanied by expansion or contraction. Note that $P \approx (1/k_T)(\Delta V/V)$, where $(\Delta V/V)$ is the fractional change in volume upon solidification. Typically, $(1/k_T) \sim 100$ GPa, and the solidification contraction is $\sim 5\%$, so the pressure P must be on the order of 5000 GPa to cause solidification. Such pressures are actually generated locally during cavitation. Many other effects of ultrasound on the solidification of castings have been observed; these include grain refinement, reduced microsegregation, root melting, improved wettability, degassing, inclusion control, etc.[52] In the solidification synthesis of cast composites, ultrasonic irradiation has been found to promote fibre infiltration and particle transfer into the melt.[58–62]

The role of pressure distribution due to cavitation on ultrasonic infiltration has been discussed by Nakanishi and co-workers.[58,59] The authors use an explicit formula obtained in Ref. 63 for the pressure P_u due to ultrasound at a point at a certain distance. For their experimental conditions, Nakanishi and co-workers found that the isobaric contours around the horn are semicircular. Ultrasonic infiltration, therefore, occurs due to the high P_u within the melt in the initial stages, but P_u tends to decrease as the infiltration front advances. These projections are consistent with the experiments.[58,59]

Other effects of pressure

A number of other effects of pressure on solidification have been identified and investigated. These include electromagnetic pressure effects,[64] MD simulations[65,66] of the effect of pressure on rapid solidification and the effect of pressure on melting and solidification of nanoparticles.[67]

Recently, the effect of hydrostatic pressure on melting and solidification at nanoscale was analysed using a thermodynamic model[68] based on the Clausius–Clapeyron equation and the size dependence of the melting entropy. The melting of nanoparticles in a matrix with coherent and incoherent boundaries was also considered. It was shown that external hydrostatic pressure yielded extrema of the melting temperature, which was a function of the characteristic size of nanoparticles.

Molecular dynamic simulation studies have been performed on the effect of pressure on the rapid solidification of Cu, Au and Al.[65,66] The microstructural evolution of bulk metals during rapid cooling under the same cooling conditions but different pressures was investigated using MD. A radial distribution function was introduced to explore the structural changes. It was revealed that the induced pressure during solidification keeps the metal in crystalline form even at very high cooling rates. Computer simulations studies[68] have been conducted on the solidification of finite metal systems ranging in size from 64 000 to 524 288 000 atoms using new computer codes. Such calculations represent atomic scale models of metal solidification under pressure from spontaneous nucleation and growth and coalescence through onset of coarsening.

Conclusions

A review of the effects of pressure on crystallisation and casting solidification was presented with a focus on the thermodynamic and kinetic aspects. The pressure effects on casting structure formation can be divided in two

groups: physical phenomena at macroscale, such as elastic or plastic deformations, intensification of heat exchange between casting and mould, variation of cooling rate, interdendritic feeding and control of mould filling; and phenomena at microscale, such as changes in phase diagrams, phase properties, Gibbs free energy, chemical potentials, specific heat, surface tension, diffusion coefficients and nucleation rate. Pressure application could significantly affect the complex physical processes during casting formation.

Explicit formulae for relationships between pressure increment and changes in some basic thermodynamic parameters of a system were obtained and discussed. It was shown that for the majority of metals and alloys, high pressure promoted structure refinement because of the following factors:

1. decreased critical radius for new phase nucleation
2. increased rate of new phase nucleation
3. decreased interfacial free energy.

The given relationships are valid for liquid–solid transformations with a negative (evolved) latent heat and negative differences of molar phase volumes, i.e. when the molar volume of solid being smaller than the molar volume of liquid. For the reverse situation, the given relationships are reversed.

At a constant temperature, high pressures increase the chemical potentials and decrease the molar entropy and diffusion coefficient, and the latter results in a higher degree of microliquation into the crystals formed.

High pressure induces many phase transformations impossible to be realised in other manner. Because of this, pressure is a unique and powerful instrument for the elaboration of new metallic materials with specific phase composition and applications. Metal matrix composites offer large possibilities in this direction because they combine properties of the matrix and the reinforcing phase appropriate for such a matrix.

References

1. P. W. Bridgman: 'The physics of high pressures'; 1931, London, G. Bell & Sons, Ltd.
2. J. D. Bernal: *Trans. Faraday Soc.*, 1929, **25**, 367–378.
3. A. S. Balchan and H. G. Drickamer: *J. Chem. Phys*., 1961, **34**, 1948.
4. R. J. Hemley: *Annu. Rev. Phys. Chem.*, 2000, **51**, 763–800.
5. A. Yuichi, H. Kawamura, D. Häusermann, M. Hanfland and O. Shimomura: *Phys. Rev. Lett.*, 1961, **74**, (23), 4690–4694.
6. S. T. Weir, A. C. Mitchell and W. J. Nellis: *Phys. Rev. Lett*., 1996, 76, 1860.
7. E. A. Guggenheim: 'Thermodynamics'; 1967, Amsterdam, Elsevier Science Publishers B.V.
8. D. A. Porter and K. E. Easterling: 'Phase transformations in metals and alloys'; 2004, Boca Raton, FL, Taylor & Francis.
9. D. Ludicke: *Z. Metallkd.*, 1986, **77**, 278–283.
10. 'Handbook of chemistry and physics', 91st edn; web version.
11. E. Brosha, G. Makov and R. Z. Shnecka: *Calphad*, 2007, **31**, 173–185.
12. A. I. Batishev: 'Solidification of metals and alloys under pressure'; 2002, Cambridge, Cambridge International Science Publishers.
13. J. Sobczak: *Trans. Foundry Res. Inst. (Poland)*, 1993, (special issue), 1–310.
14. T. N. Lipchin: *Liteynoe Proizvodstwo (Russia)*, 1985, **7**, 9–10.
15. J. Sobczak, D. Rudnik, N. Sobczak, A. Wojcichowski and K. Pietrzak: *Trans. JWRI*, 2001, **30**, 455–462.
16. D. Kashchiev and G. M. van Rosmalen: *J. Colloid Interf. Sci.*, 1995, **169**, (1), 214–219.
17. S. Vasudevan, S. Nagalingam, P. Ramasamy and G. S Laddha: *Cryst. Res. Technol.*, 1979, **14**, (4), 373–490.
18. W.-L. Huang: *Eur. J. Mineral.*, 2003, **15**, 843–853.
19. J. Wedekind, A.-P. Hyvärinen, D. Brus and D. Reguera: *Phys. Rev. Lett.*, 2008, **101**, 125703.
20. H. Mehrer and A. Seeger: *Cryst. Latt. Def*., 1972, **3**, 1.
21. R. H. Dickerson, R. C. Lowell and C. T. Tomizuka: *Phys. Rev. A*, 1965, **613A**, 137.
22. J. N. Mundy: *Phys. Rev. B*, 1971, **3B**, 2431.
23. M. Werner, H. Mehrer and H. D. Hochheimer: *Phys. Rev. B*, 1985, **32B**, 3930.
24. M. J. Aziz, E. Nygren, W. H. Christie, C. W. White and D. Turnbull: in 'Impurity diffusion and gettering in silicon', Proc. MRS Symp., (ed. R. B. Fair *et al.*), Vol. 36, 101; 1985, Pittsburgh, PA, MRS.
25. S. Mitha: 'The effect of pressure on arsenic diffusion in germanium', PhD thesis, Harvard University, Cambridge, MA, USA, 1995.
26. Y. Arsov, E. Momchilov, K. Daskalov and G. Bachvarov: 'Theoretical and technological fundamentals of gas counter-pressure casting'; 2007, Sofia, Prof. Marin Drinov Academic Publishing House.
27. J. Sobczak: 'Kompozyty Metalowe'; 2001, Cracow, Institute Odlewnictwa.
28. R. Asthana: 'Solidification processing of reinforced metals'; 1998, Zurich, Trans Tech.
29. J. Sobcak, N. Sobczak, R. Asthana, A. Wojciechowski, K. Pietrzak and D. Rudnik: 'Atlas of cast metal–matrix composite structures', 144; 2007, Warsaw, Motor Transport Institute/Krakow, Foundry Research Institute.
30. J. Sobczak, Z. Slawinski, N. Sobczak, P. Darlak, R. Asthana and P. K. Rohatgi: *J. Mater. Eng. Perform.*, 2002, **11**, (6), 595–602.
31. J. Bienias, M. Walczak, B. Surowska and J. Sobczak: *J. Optoelectron. Adv. Mater.*, 2003, **5**, (2), 493–502.
32. L. B. Drenchev and J. Sobczak: Proc. Int. Conf. on 'High-temperature capillarity', (ed. N. Eustathopoulos and N. Sobczak), 349–354; 1997, Krakow, Foundry Research Institute.
33. J. A. Sekhar, G. J. Abbaschian and R. Mehrabian: *Mater. Sci. Eng.*, 1979, **40**, (1), 105–110.
34. L. Drenchev and J. Sobczak: Proc. 2nd Int. Conf. on 'High temperature capillarity', (ed. N. Eustathopoulos and N. Sobczak), 355–361; 1997, Krakow, Foundry Research Institute.
35. L. Drenchev and J. Sobczak: Proc. 2nd Int. Conf. on 'High temperature capillarity', (ed. N. Eustathopoulos and N. Sobczak), 355–361; 1997, Krakow, Foundry Research Institute.
36. D. J. Britnell and K. Neailey: *J. Mater. Process. Technol.*, 2003, **138**, 306–310.
37. L. Drenchev, J. Sobczak, N. Sobczak, W. Sha and S. Malinov: *Acta Mater.*, 2007, **55**, (19), 6459–6471.
38. L. C. LaCombe, M. B. Koss, L. A. Tennenhouse, E. A. Winsa and M. E. Glicksman: *J. Cryst. Growth*, 1998, **194**, 143–148.
39. C. A. Jeffery and P. H. Austin: *J. Geophys. Res.*, 1997, **102**, (D21), 25269–25280.
40. T. N. Lipchin et al.: 'Modern methods for obtaining of ingots and materials', in 'Progresivnie metodi poluchenia zagotovok i materialov', Vol. 131, 85–90; 1973, Perm, PPI.
41. R. Gavrilova, V. Manolov, A. Yotova, S. Popov and L. Saraivanov: in Proc. 4th Int. Cong. on 'Mechanical engineering technologies', Varna, Bulgaria, September2004, Vol. 3/71, 135–137.
42. D. He, M. He, C. S. Kiminami, F. X. Zhang, Y. F. Xu, W. K. Wang and K. H. Kuo: *J. Mater. Res.*, 2001, **16**, (4), 910–913.
43. P. W. Zhu, L. X. Chen, X. Jia, H. A. Ma, G. Z. Ren, W. L. Guo, H. J. Liu and G. T. Zou: *J. Phys. Condens. Matter*, 2002, **14**, 11011–11015.
44. B. Yao, H. C. Guo, J. Wang, B. Z. Ding, H. Li, A. M. Wang and Z. Q. Hu: *Physica B*, 1996, **228B**, 379–382.
45. J. Zhang, K. Qiu, A. Wang, H. Zhang, M. Quan and Z. Hu: *J. Mater. Sci. Technol.*, 2004, **20**, (1), 106–108.
46. B. Suarez-Pena, J. Asensio-Lozano and G. F. Vander Voort: *Microsc. Microanal.*, 2007, **13**, (2), 1030–1031.
47. C.-H. Wu, M. Qureshi and C.-H. Lu: *J. Phys. Chem. Solids*, 2008, **69**, 475–479.
48. A. Kagawa, T. Imaizumi and M. Mizumoto: *Mater. Trans.*, 2001, **42**, (7), 1385–1391.
49. H. A. Ma, X. P. Jia, L. X. Chen, P. W. Zhu, W. L. Gou, X. B. Guo, Y. D. Wang, S. Q. Li, G. T. Zou, G. Zhang and P. Bex: *J. Phys. Condens. Matter*, 2002, **14**, 11269–11273.
50. H. A. Ma, X. P. Jia, L. X. Chen, P. W. Zhu, G. Z. Ren, W. L. Guo, X. Q. Fu, G. T. Zou, Z. A. Ren, G. C. Che and Z. X. Zhao: *J. Phys. Condens. Matter*, 2002, **14**, 11181–11184.

51. P. W. Zhu, L. X. Chen, X. Jia, H. A. Ma, G. Z. Ren, W. L. Guo, W. Zhang and G. T. Zou: *J. Phys. Condens. Matter*, 2002, **14**, 11185–11188.
52. J. Campbell: *Int. Met. Rev.*, 1981, **2**, 71–108.
53. L.-Q. Ma, G.-J. Shu and F. Chen: *Mater. Sci. Eng.*, 1995, **13**, (4), 2–7.
54. J. Li, W. Chen, Q. Liu and X. Wang: *Steel Res. Int.*, 2008, **79**, (5), 358–363.
55. B. E. Noltingk and E. A. Neppiras: *Proc. Phys. Soc. B*, 1950, **63B**, 674.
56. B. E. Noltingk and E. A. Neppiras: *Proc. Phys. Soc. B*, 1951, **64B**, 1032.
57. L.-Q. Ma, G.-J. Shu and F. Chen: *J. Mater. Sci. Lett.*, 1995, **14**, 649–650.
58. H. Nakanishi, Y. Tsunekawa, M. Okumiya and N. Mohri: *J. Mater. Sci. Lett.*, 1993, **12**, 1313–1315.
59. Y. Tsunekawa, H. Nakanishi, M. Okumiya and N. Mohri: *AFS Trans.*, 1994, **102**, 953–958.
60. Y. Deming, Y. Xinfang and P. Jin: *J. Mater. Sci. Lett.*, 1993, **12**, 252.
61. B. Sartor, H. Staats and H. J. Seeman: *Metall.*, 1974, **28**, 771.
62. J. Pan, D. M. Yang, X. F. Liu and H. Fukunaga: *J. Mater. Res.*, 1995, **10**, (3), 596.
63. K. U. Ingard: 'Fundamentals of waves and oscillations', 315; 1988, Cambridge, Cambridge University Press.
64. T. Masahiro, T. Eiichi, F. Takehiko and K. Kiyoshi: 'New advancements in electromagnetic processing of materials', 113–116; 1999.
65. J. Liu, J. Z. Zhao and Z. Q. Hu: *Comput. Mater. Sci.*, 2006, **37**, 234.
66. Y. N. Zhang, L. Wang, W. M. Wang, X. F. Liu, X. L. Tian and P. Zhang: *Phys. Lett.*, 2004, **320**, 452.
67. A. P. Chernyshev: *Phys. Lett.*, 2009, **373**, 1070–1073.
68. F. H. Streitz, J. N. Glosli, M. V. Patel, B. Chan, R. K. Yates, B. R. de Supinski, J. Sexton and J. A. Gunnels: *J. Phys. Conf.*, 2006, **46**, 254–267.